Relationship among thermal anomalies, superconductivity and structural blocks in different-metal-site-doped YBCO

2008 J. Phys.: Condens. Matter 20 075209

(http://iopscience.iop.org/0953-8984/20/7/075209)

J. Phys.: Condens. Matter **20** (2008) 075209 (8pp) doi:10.1088/0953-8984/20/7/075209

Relationship among thermal anomalies, superconductivity and structural blocks in different-metal-site-doped YBCO

L Zhang[1,2,3], X F Sun[2], Y Z Wang[2], H L Du[2] and H Zhang[2]

[1] School of Science, China Jiliang University, Hangzhou 310018, People's Republic of China
[2] Material Physics Laboratory, State Key Laboratory for Mesoscopic Physics, Department of Physics, Peking University, Beijing 100871, People's Republic of China

E-mail: Lzhang@cjlu.edu.cn

Received 29 August 2007, in final form 2 January 2008
Published 28 January 2008
Online at stacks.iop.org/JPhysCM/20/075209

Abstract

Three series of polycrystalline samples of $YBa_2Cu_{3-x}Ni_xO_y$ (YBCNO), $Y_{1-x}Pr_xBa_2Cu_3O_y$ (YPrBCO) and $YBa_{2-x}La_xCu_3O_y$ (YBLCO) ($x = 0, 0.05, 0.10, 0.15, 0.20, 0.25$, respectively), synthesized by a solid state reaction technique, were characterized by thermogravimetry, differential scanning calorimetry, DC magnetization measurement, temperature dependent x-ray diffraction and Rietveld refinement. To our knowledge this is the first systematic report of two phase transitions at about 400 and 850 °C before melting. By careful measurements it was seen that the amounts of the percentage weight loss and the DSC changes, along with T_c, decrease with increasing dopant. Combining the theory of oxygen diffusion with the block model in YBCO, the mechanism of the phase transitions can be explained as follows: the phase transition at 400 °C comes directly from O(1) in the rock salt block, while the phase transition at 850 °C is related to the perovskite block. The calculation of the combinative energy between the two structural rock salt and perovskite blocks shows that, with increasing dopant, the higher the combinative energy the lower the T_c, and vice versa. The results indicate that there exits a triangular relationship among thermal anomalies, superconductivity and structural blocks in different-metal-site-doped YBCO, which may be significant for understanding the mechanism of high-temperature superconductivity.

(Some figures in this article are in colour only in the electronic version)

1. Introduction

Since the discovery of high-temperature (T_c) superconductors (HTSCs), significant progress has been made in understanding their mechanism. The most important advance has been the electronic phase diagram [1], based on the relationship between superconductivity and carrier concentration. The diagram clearly shows the effect of carrier concentration on the superconductivity, but as the concentration changes, the crystalline structure changes simultaneously. However, it is still insufficient for understanding the influence of structural factors on the superconductivity. The fundamental HTSC is a Mott insulator in a Cu-atom anti-ferromagnetic background. As always, the crystal cell is formed in two ways [2]: stacked simply or stacked with a translation vector $1/2(\mathbf{a} + \mathbf{b})$, though a little oxygen becomes lost in some sites. This demonstrates that the crystalline structure plays an important role in the mechanism of superconductivity. A study of the effects of structural factors on the superconductivity, which can enrich the meaning of the electronic phase diagram from another aspect, is thus significant for exploring the mechanism of HTSC.

Zhang *et al* [3–5] reported that $YBa_2Cu_3O_7$ (YBCO) exhibits an endothermal anomaly and weight loss at about 300 °C, while PrBCO shows an exothermal anomaly and weight gain at about the same temperature. Because superconducting YBCO is isostructural with non-superconducting PrBCO, the anomaly at 300–400 °C may imply something interesting for superconductivity. Moreover, it was observed that

[3] Author to whom any correspondence should be addressed.

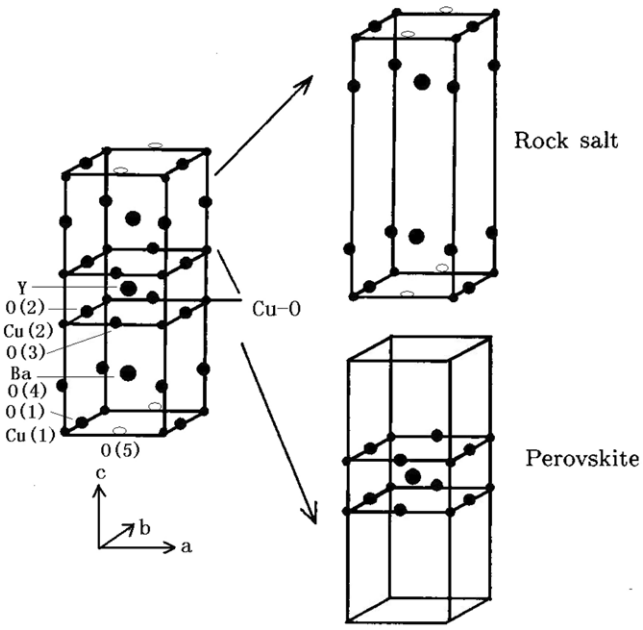

Figure 1. The common structure of YBCO systems. The structure can be divided into two blocks, perovskite and rock salt.

there are two thermal anomalies at about 300 and 700 °C, respectively, in Bi systems [6]. It is therefore worthwhile to pay more attention to the relationship between thermal anomalies and superconductivity in HTSCs. What is the origin of the thermal anomalies? Do they have something to do with superconductivity? If so, is the correlation specific to YBCO or is it common to all HTSCs?

On the other hand, HTSCs demonstrate strong two-dimensional characteristics; the coupling along the *c* direction in the crystals is of great importance. This characteristic has been studied extensively [7, 8]. In most of these studies, HTSCs are regarded as a multilayer with superconducting and non-superconducting layers. Coupling between the superconducting layers is also considered. However, the role played by different layers in the electronic properties in normal states is not very clear. As there are many layers along the *c* direction in HTSCs, it will be difficult to deal with the coupling between all the planes. However, if we can reasonably divide these layers into a few blocks based on their structural characteristics and the experimental facts, the problem will be easier. Recently, Zhang *et al* [9–11] developed a model based on the fact that in HTSCs the unit cell can be divided into two different blocks: one is perovskite, the other is rock salt. The perovskite block is the active block where the Cu(2)–O planes are located and the carriers are concentrated. The rock salt block is the so-called reservoir block, which provides carriers to the Cu(2)–O planes. The division of the two blocks is shown in figure 1.

In this paper, from the structural viewpoint, high-temperature thermal analyses and high-temperature x-ray diffraction are combined to investigate the relationship among the thermal transitions, superconductivity and the two different blocks in different-metal-site-doped YBCO systems such as $YBa_2Cu_{3-x}Ni_xO_y$, $Y_{1-x}Pr_xBa_2Cu_3O_y$ and $YBa_{2-x}La_xCu_3O_y$ with the help of Rietveld refinement and combinative energy calculation.

2. Experiment

The compounds of $YBa_2Cu_{3-x}Ni_xO_y$, $Y_{1-x}Pr_xBa_2Cu_3O_y$ and $YBa_{2-x}La_xCu_3O_y$ ($0 \leqslant x \leqslant 0.25$) were synthesized via a solid state reaction route. The samples were investigated by temperature dependent XRD, Rietveld refinement, thermal analyses and magnetic moment–temperature measurement. Thermal analyses were carried out on a Rheometric Scientific STA 1500 thermoanalyzer capable of simultaneous differential scanning calorimetry (DSC) and thermogravimetry (TG) analyses. Each powder sample, with a weight of about 50 mg, was analyzed in an Al_2O_3 crucible. The heating rate was 10 °C min^{-1} in an argon atmosphere. Temperature dependent x-ray powder analysis was performed on a Philips X'pert Pro MPD diffractometer with by Cu Kα radiation in a vacuum (10^{-2}–10^{-3} Pa). Detailed structural characteristics were obtained by Rietveld refinement [12] using the X'pert Plus software. The goodness of fit (GOF $= R_{wp}/R_{exp}$) of all samples at different temperatures is about 1.5, demonstrating that the refinement results are reliable. The T_c was determined by a Quantum Design MPMS system between 20 and 120 K at an external field of $H = 10$ Oe.

3. Results and discussion

3.1. The qualities of three doped YBCO systems

As YPrBCO is a transition from YBCO (superconducting) to PrBCO (non-superconducting), the YPrBCO system has been used as a research tool for a better understanding the mechanism of HTSC [13–15]. Pr-doped YBCO was selected to represent the Y-site substitution. Ni^{2+} has almost the same valence and ionic radius as Cu^{2+} and a Cu(2)–O plane plays a key role in HTSCs. Thus Ni dopants suppress superconductivity significantly [16, 17]. As for La-doped YBCO, La^{3+} in place of Ba^{2+} is a classical non-isovalent substitution in YBCO systems, which results in the changes of oxygen content, structure and carrier concentration [18–20].

Figures 2(a)–(c) show the XRD profiles at room temperature, 400 and 850 °C for $x = 0.05$ Ni-, Pr- and La-doped YBCO systems, respectively. All the peaks in each pattern can be indexed with the symmetry of *Pmmm*, demonstrating that the samples exhibit single phases within the resolution of the diffractometer. The DC magnetization measurements indicate that there are no phase separation phenomena in any of the samples. The values of T_c decrease with Ni-, Pr- and La-dopant increase, as shown in figure 3. The Ni^{2+} substitution for Cu^{2+} gives a greater depression of the superconductivity than that of Pr^{3+} and La^{3+}, demonstrating the importance of the Cu(2)–O plane in HTSCs.

3.2. Thermal analysis and two phase transitions

Thermal analysis was carried out on all the samples from room temperature to 1000 °C. Two thermal anomalies were observed at about 400 and 850 °C, characterizing the Ni-doped YBCO

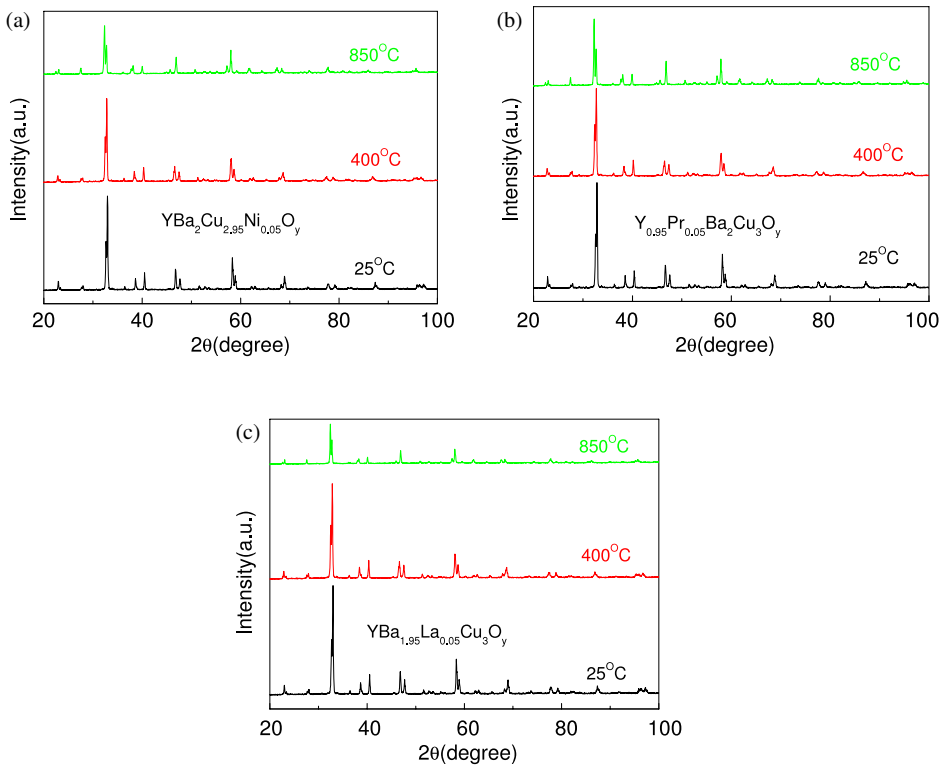

Figure 2. The XRD profiles of the three doped YBCO systems at room temperature, 400 and 850 °C, respectively: (a) Ni-doped sample ($x = 0.05$); (b) Pr-doped sample ($x = 0.05$); (c) La-doped sample ($x = 0.05$). The results of peak indexing demonstrate that the samples are still in an orthorhombic phase at 400 °C, but have undergone an O–T phase transition below 850 °C.

heated in an argon atmosphere. In figure 4(a) two endothermal anomalies are evident at about 400 and 850 °C. In figure 4(b) two weight loss anomalies can be observed corresponding to the two endothermal anomalies. By careful measurements, it was found that the DSC changes and the percentage weight loss have a close relationship with the change of T_c value, i.e. with the increasing values of Ni content x, both the changes of DSC and the percentage weight loss, along with T_c, decrease. Similar phenomena were observed in the Pr- and La-doped YBCO systems. To our knowledge this is the first time that two phase transitions in doped YBCO have been reported and linked to changes in T_c.

There exists an endothermal anomaly and a weight loss at about 300 °C in YBCO, compared with an exothermal anomaly and weight gain at about 400 °C in PrBCO. Both YBCO and PrBCO are almost the same in structure but different in superconductivity. Their opposite thermal anomalies at about 300–400 °C may reveal something interesting about their superconducting properties. A thermal analyzer–mass spectrometer connecting system was used by Zhang *et al* [3, 6] to determine the weight change of the YBCO in a vacuum (10^{-4}–10^{-5} mbar) from room temperature to the melting point. It was observed that a small quantity of oxygen was emitted from the YBCO samples at 350–450 °C and 750–850 °C, suggesting that the two anomalies shown in the DSC and TG curves are accompanied by a loss of oxygen in YBCO. We suggest that the situation is the same in the three doped YBCO systems.

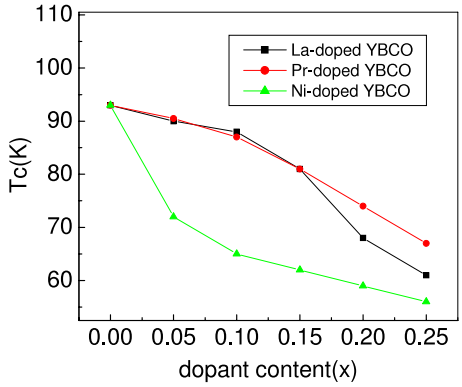

Figure 3. T_c versus doping content x in the Ni-, Pr- and La-doped YBCO systems.

Cava *et al* reported a similar phenomenon in $YBa_{2-x}La_xCu_3O_y$ ($0 \leqslant x \leqslant 0.25$) [21].When the La content (x) is 0.05, 0.10, 0.15 and 0.20, respectively, the corresponding percentage oxygen loss is 1.90, 1.80, 1.60 and 1.50 at 400 °C heated in oxygen, and the corresponding percentage oxygen loss is 1.90, 1.90, 1.70 and 1.50 at 850 °C heated in nitrogen. Unfortunately, no further information or explanation were given about this phenomenon. The detailed DSC changes and percentage weight loss of the three doped YBCO systems are depicted in figures 5(a) and (b). From these, both the DSC changes and percentage weight loss in the Ni-doped YBCO are

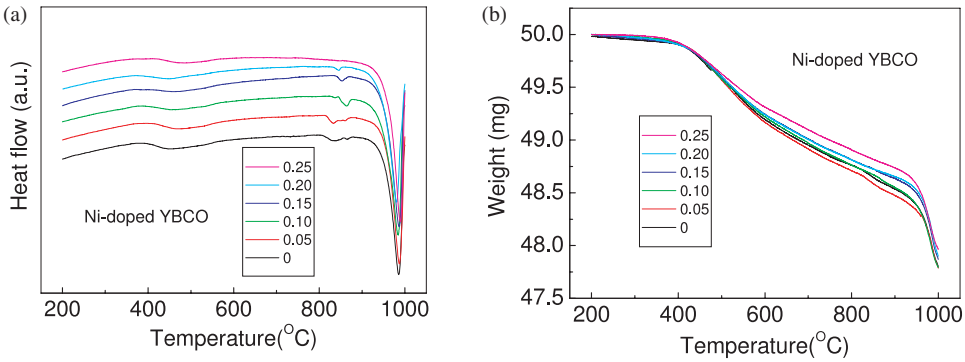

Figure 4. (a) DSC curves of Ni-doped YBCO heated in an argon atmosphere. Two heat flow anomalies are obvious at about 400 and 850 °C. (b) TG curves of Ni-doped YBCO heated in an argon atmosphere. Two weight anomalies are detected at about 400 and 850 °C corresponding to the DSC curve.

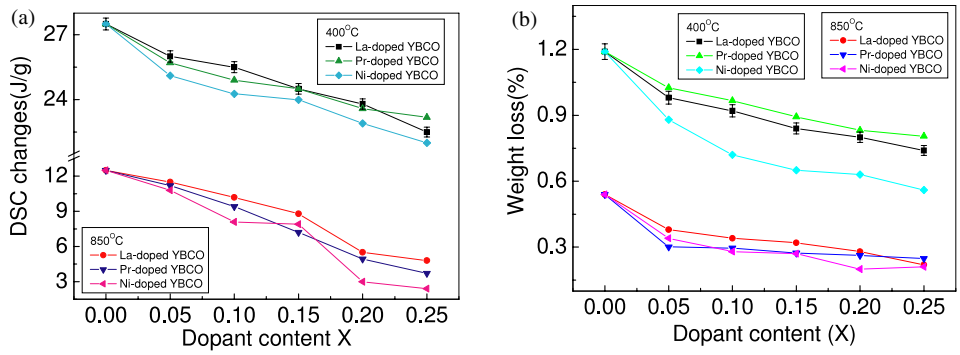

Figure 5. (a) DSC changes in Ni-, Pr-, and La-doped YBCO at about 400 and 850 °C. The three doped systems have a similar behavior: the DSC changes decrease with increasing dopant. (b) Relative weight loss in Ni-, Pr-, and La-doped YBCO at about 400 and 850 °C. The three doped systems also have a similar behavior: the relative weight losses decrease with increasing dopant.

greater at 400 °C than in the Pr- and La-doped YBCO, which is consistent with the reduction in the T_c value in figure 3.

Jorgensen *et al* [22] reported there is an O–T structural transition at about 700 °C in YBCO. By comparing the characteristics of the O–T transition of YBCO with the anomalies described above at 400 and 850 °C for the three doped YBCO systems, some interesting differences and similarities can be seen, as described below: (1) both the O–T transition and the anomalies at 400 and 850 °C involve the loss of weight, i.e. loss of oxygen. (2) Both the anomalies at 400 and 850 °C show a heat change, which has never been observed in the O–T transition. (3) The O–T transition originates from the order–disorder transition of oxygen located in the Cu(1)–O chain layer. The space group of the orthorhombic structure is $Pmmm$, whereas the space group of the tetragonal structural is $P4/mmm$, which is a supergroup of $Pmmm$. The O–T transition is a second-order phase transition. This is different from the anomalies at 400 and 850 °C, which are first-order phase transitions as shown by the DSC change during the transition. Moreover, no detectable changes can be found in the crystal symmetry in the anomalies at 400 and 850 °C.

There are two ways for oxygen to diffuse in a YBCO system. One is the rearrangement of oxygen in the crystal cell (short distance diffusion) and the other is the entering into or escape from the O(1) site (long distance diffusion). In the YBCO system, oxygen in the Cu(1)–O plane or Cu–O chain is easily lost. For example, energy of 1.7 eV will be needed to bring two oxygen atoms from crystal and to make them form a molecule and escape from the surface of the sample. In addition, YBCO is annealed at 370–400 °C for about 10–20 h for oxygen atoms to enter into O(1) sites; however, there are no oxygen atoms lost in the Cu(2)–O plane at this temperature. This indicates more energy needed to destroy the bond lengths or form oxygen holes on the Cu(2)–O plane [23]. Combining the mechanism of oxygen diffusion in YBCO with the block model, the mechanism of the phase transitions can be explained as follows: the phase transition at 400 °C comes directly from O(1) in the rock salt; the phase transition at 850 °C corresponds to O(2) and O(3) in the Cu(2)–O plane. When the second phase transition takes place, the occupancy of oxygen at O(2) and O(3) sites is adjusted and a few oxygen atoms enter the O(1) sites of the Cu(1)–O plane through O(4) bridge atoms, finally escaping from the crystal cell and causing the phase transition at 850 °C to take place. This is related to the perovskite block.

3.3. XRD results and Rietveld refinement

Temperature dependent XRD was used to determine whether the phase transition at 400 °C comes directly from O(1) in the

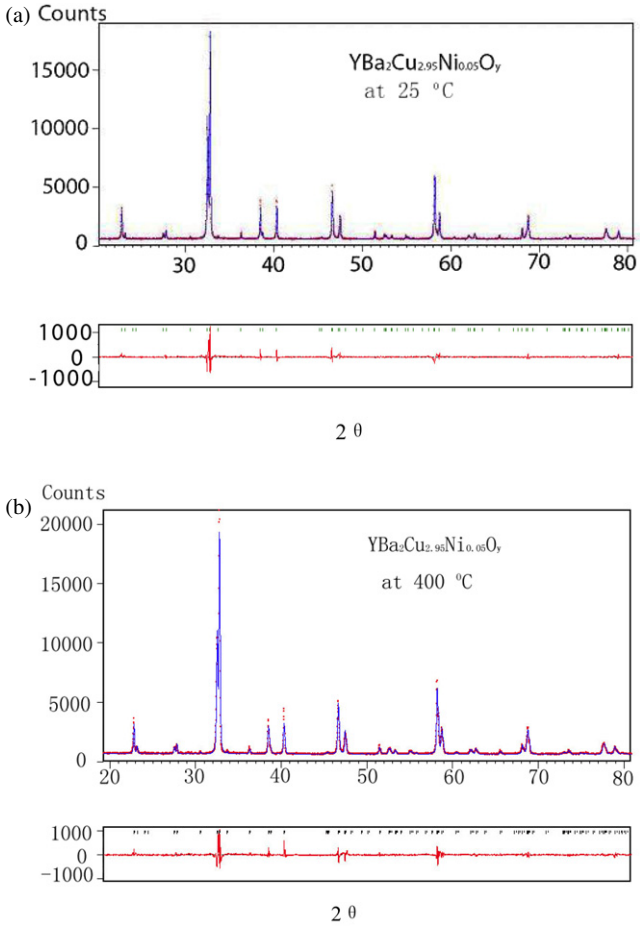

Figure 6. (a) Refinement profiles of $YBa_2Cu_{2.95}Ni_{0.05}O_y$ at room temperature. The dotted line is the measurement result and the solid line is the calculated profile. The vertical short line represents the position of Bragg reflection. The difference curves are plotted at the bottom. (b) Refinement profiles of $YBa_2Cu_{2.95}Ni_{0.05}O_y$ above 400 °C, indicating that the samples were still in a single orthorhombic phase, but the crystalline parameters have changed a little above 400 °C. The dotted line is the measurement result and the solid line is the calculated profile. The vertical short line represents the position of Bragg reflection. The difference curves are plotted at the bottom.

rock salt block, and the phase transition at 850 °C is related to the perovskite. Figure 6(a) shows the XRD profiles and refined results for $YBa_2Cu_{2.95}Ni_{0.05}O_y$ at room temperature. Figure 6(b) plots the XRD profiles and refined results for $YBa_2Cu_{2.95}Ni_{0.05}O_y$ at 400 °C. The results of peak indexing demonstrate that the samples are still in the orthorhombic phase at 400 °C. All the samples have undergone an O–T transition below 850 °C, a temperature far lower than that for pure YBCO in a vacuum [24]. We attribute this to the Ni dopant, which enhances the O–T transition when the sample is heated.

Rietveld refinement was carried out with the same atomic proportions of Y, Ba, Cu, and Ni as in the ingredients. The occupancy of O(2), O(3) and O(4) is supposed to be 1. The goodness of the fit is about 1.5. The changes in the three crystalline parameters (a, b, c) are consistent with the previous results [16, 17], obtained from neutron diffraction or XRD, showing that our refinement results are reliable. Similar analyses can be performed on the Pr- and La-doped YBCO. Table 1 shows some selected bond lengths in Ni-doped YBCO at room temperature and at about 400 °C obtained from the Rietveld refinement. After the first thermal transition, the Ba–O(2) and Ba–O(3) bond lengths, located in the rock salt block, become much longer than those in the perovskite block. For example, the Ba–O(2) bond length in YBCNO ($x = 0.05$) varies from 2.9013 to 2.9681 Å with an absolute change of 0.0668 Å and relative change of 2.3%. The corresponding values of Ba–O(3) are 2.9868 Å, 3.0362 Å, 0.0494 Å and 1.7%, respectively. However, the bond lengths of Y–O(2), Y–O(3), Cu(2)–O(2) and Cu(2)–O(3) are almost unchanged. Thus, the anomaly at about 400 °C is identified to be due to the rock salt block.

For the other anomaly, because the O–T transition occurred below 850 °C, it is difficult to compare the changes of bond length when the second phase transition occurs. Based on the theory of oxygen diffusion, the oxygen occupancy ratio at each site is rearranged when the temperature increases. At about 400 °C, some oxygen escapes from the rock salt block, as demonstrated by the thermal analyzer–mass spectrometer connecting system and the calculation of the bond lengths (see table 1). As the temperature gradually increases, the remaining oxygen has to be rearranged to match the two blocks and to stabilize the unit cell. The oxygen at the O(2) and O(3) sites may move to O(1) and O(5) though the 'bridge' atom oxygen O(4), then some of them escape from the crystal cells via the O(1) site. The second phase transition correlates reasonably well with the perovskite block.

3.4. Calculation of combinative energy

The interaction between perovskite and rock salt blocks is measured by means of the combinative energy, which is defined as the combinative energy between the two blocks, and is equal to the cohesive energy of the whole cell minus the cohesive energy of the perovskite block minus the cohesive energy of the rock salt block. The combinative energy between the two blocks in YBCO systems was calculated by a computer program developed by ourselves. According to the classical theory, the cohesive energy of the crystal can be written as a sum of the Madelung energy E_M, the repulsive energy of ions E_r, and the electron affinity energy E_a, namely,

$$E_n = E_M + E_r + E_a \tag{1}$$

and

$$E_M = 1/2c \sum e_i e_j / r_{ij}, \tag{2}$$

$$E_r = a e^{-1/\rho}, \tag{3}$$

$$E_\alpha = \sum \sum \varepsilon_{ij}. \tag{4}$$

Here e_i and e_j are the electric charges of the different ions, r is the distance between two different ions, and ε_{ij} is the ionization energy if the j atoms in the cell and a is proportional to the coefficients (such as ionic radio and the electric charges in the outer shell). We discard the electron affinity energy

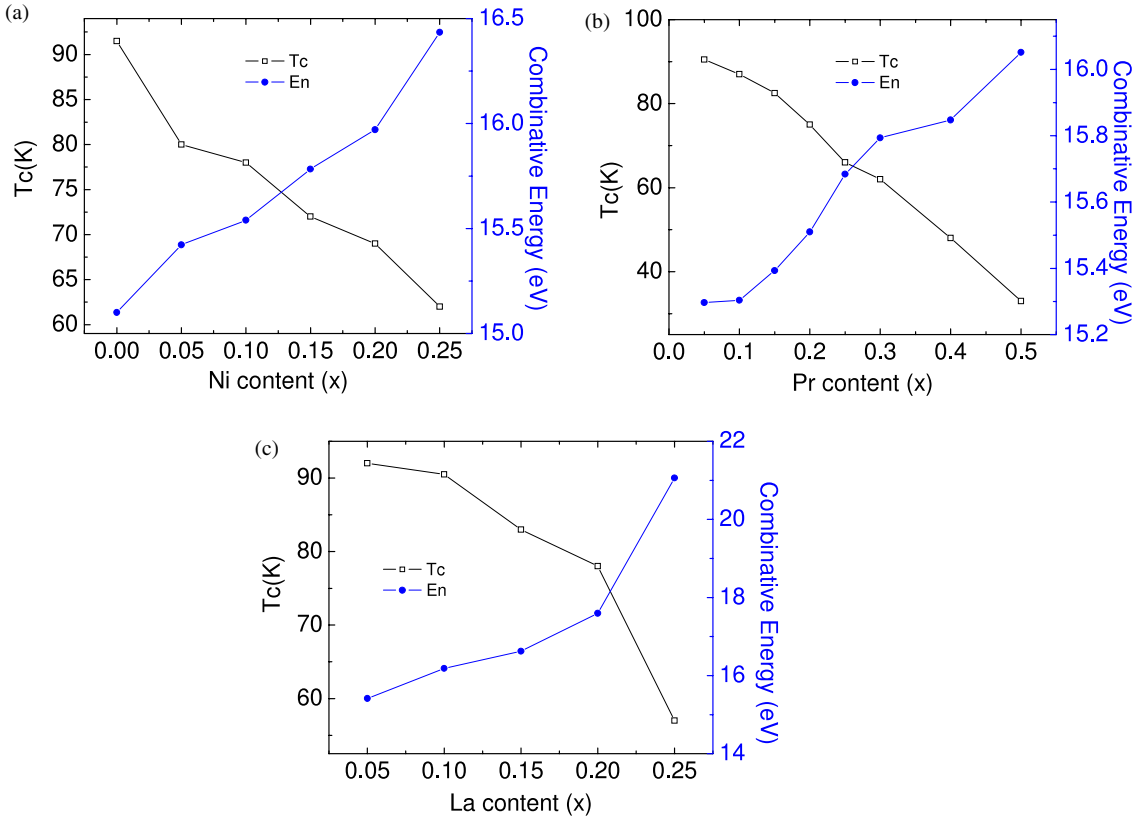

Figure 7. The combinative energy between perovskite and rock salt blocks versus T_c in (a) Ni-doped samples, (b) Pr-doped samples, and (c) La-doped samples.

Table 1. Selected bond lengths (BL) (Å) determined by Rietveld refinement in pure YBCO and three different-metal-site-doped YBCO systems ($x = 0.05$). The symmetry is still $Pmmm$ after the first transition (at about 400 °C) and changes to $P4/mmm$ after the second transition (at about 850 °C). The atomic position was defined as follows: Y/Pr (1/2, 1/2, 1/2), Ba/La (1/2, 1/2, z), Cu2/Zn (0, 0, z), O4 (0, 0, z), O2 (0, 1/2, z), O3 (1/2, 0, z), the same as defined in figure 1.

BL (Å)	Y–O(2)	Y–O(3)	Ba–O(2)	Ba–O(3)	Cu(2)–O(2)	Cu(2)–O(3)
Pure YBCO						
25 °C	2.425	2.406	2.915	2.986	1.956	1.937
400 °C	2.397	2.431	3.087	2.879	1.979	1.924
$BL_{25\,°C}$–$BL_{400\,°C}$	0.028	−0.025	−0.172	0.107	−0.023	0.013
$(BL_{25\,°C}–BL_{400\,°C})/BL_{25\,°C}$	0.012	−0.010	−0.059	0.036	−0.012	0.007
La-doped YBCO						
25 °C	2.437	2.389	2.873	3.014	1.951	1.948
400 °C	2.397	2.428	3.003	2.934	1.978	1.934
$BL_{25\,°C}$–$BL_{400\,°C}$	0.040	−0.039	−0.130	0.080	−0.027	0.014
$(BL_{25\,°C}–BL_{400\,°C})/BL_{25\,°C}$	0.016	−0.016	−0.045	0.026	−0.014	0.007
Pr-doped YBCO						
25 °C	2.402	2.414	2.945	2.981	1.960	1.932
400 °C	2.384	2.433	3.106	2.898	2.003	1.933
$BL_{25\,°C}$–$BL_{400\,°C}$	0.018	−0.019	−0.161	0.083	−0.043	−0.001
$(BL_{25\,°C}–BL_{400\,°C})/BL_{25\,°C}$	0.007	−0.008	−0.055	0.028	−0.022	−0.0005
Ni-doped YBCO						
25 °C	2.4358	2.4078	2.9013	2.9868	1.9528	1.9330
400 °C	2.4046	2.3824	2.9681	3.0362	1.9633	1.9430
$BL_{25\,°C}$–$BL_{400\,°C}$	0.031	−0.025	−0.067	−0.049	−0.010	0.010
$(BL_{25\,°C}–BL_{400\,°C})/BL_{25\,°C}$	0.013	0.010	−0.023	−0.017	−0.005	0.005

since once the atom becomes an ion, the ion has a closed shell and the electron affinity energy will have little effect on other electrons or vacancies. Some authors have demonstrated that the ion model can be used to deal with high-temperature superconductors [25, 26]. We use the ionic model to simplify the problem. To make the calculation more precise and the

model more reasonable, the covalence is also approximately considered. To calculate the Madelung energy, we use the standard Evjen method [27] in which the distribution of the charges in a cell is balanced and the summation is highly convergent. To calculate the repulsive energy, we use a Bohr approximation. The accuracy and reliability of the calculation method have been well tested by Zhang *et al* [9–11] in Ln (Ln = Y, Nd, Er, Sm)BCO, LaMCO (M = Ba, Sr), Bi- and Hg-system HTSCs.

But as far as doped HTSC is concerned, the combinative energy has not been calculated before. In order to better understand the influence of structure on superconductivity, the combinative energy between the two blocks in three doped YBCO systems at room temperature was calculated. Figures 7(a)–(c) support the conclusion: the higher the combinative energy between the two blocks, the lower T_c, and vice versa. We suggest the reason is that the smallest energy corresponds to the most stable state in the crystal, or the best state in the structure, and therefore is consistent with the highest T_c value. With the dopant increasing, the match between the two blocks is reduced gradually, and in the meantime the combinative energy becomes bigger and therefore the T_c value becomes smaller.

4. Conclusions

In summary, from the structural viewpoint, three different-metal-site-doped YBCO systems were investigated by means of TG and DSC analysis, high resolution x-ray diffraction at room temperature and high temperature with the help of Rietveld refinement and combinative energy calculation. The following conclusions may be made:

(1) Discovery of phase transitions. To our knowledge this is the first report of two phase transitions at about 400 and 850 °C in each sample before melting.

(2) Explanation of phase transitions. Combining the theory of oxygen diffusion with the block model, the phase transitions can be explained as follows: the phase transition at 400 °C comes directly from O(1) in the rock salt, while the phase transition at 850 °C corresponds to the perovskite block.

(3) Relationship between phase transition and T_c. The amount by which the DSC changes and the percentage weight loss are related to T_c, whether at a temperature of 400 or 850 °C. With increase in the dopants, the T_c value and the changes in TG and DSC decrease.

(4) Combinative energy calculation. The combinative energy between the two structural blocks in the three systems are calculated according to the block model. The results extend the conclusion in pure HTSCs to doped YBCO systems: the higher combinative energy between the two blocks, the lower T_c, and the opposite is also existed. The reason may be that the smallest combinative energy corresponds to the most stable state in the crystal, or the best state in the structure, therefore is consistent with the highest T_c value.

On the whole, the two phase transitions at 400 and 850 °C in doped YBCO systems are related to the two structural blocks, and are consistent with the T_c value; the combinative energy between the two structural blocks is also consistent with the T_c value. There exits a triangular relationship among thermal anomalies, superconductivity and structural blocks in the three different-metal-site-doped YBCO systems. The changes in crystal structure, especially the changes in oxygen structure, lead to changes in the combinative energy between the two structural blocks, and thus the T_c value at room temperature, and then to the phase transitions at high temperature. This deserves further discussion.

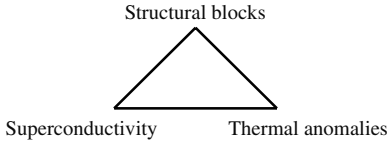

References

[1] Orensteinl J and Millis A J 2000 *Science* **288** 468
[2] Park C and Snyder R L 1995 *J. Am. Ceram. Soc.* **78** 3171
[3] Zhang H, Feng Q R, Feng S Q, Ritter F and Assmu W 1996 *J. Phys.: Condens. Matter* **8** 3653
[4] Zhang L, Yu L P, Zhang W, Wang Y Z, Zhang H and Zhao Y 2001 *Physica* C **357–360** 194
[5] Zhang L, Zhang W and Zhang H 2001 *Physica* C **364/365** 420
[6] Zhang H, Zhao Y, Feng Q R, Ritter F and Assmus W 1997 *Physica* C **284** 879
[7] Kleiner R, Steinmeyer F, Kunkel G and Muller P 1992 *Phys. Rev. Lett.* **68** 2394
[8] Zhao Y, Gu G D, Russel G R, Nakamura N, Tajima S, Wei J G, Uehara K and Koshizuka N 1995 *Phys. Rev.* B **51** 3134
[9] Zhang H, Cheng L L, Qin X C and Zhao Y 2000 *Phys. Rev.* B **61** 1618
[10] Zhang H, Cheng L L and Zhao Y 2000 *Phys. Rev.* B **62** 13907
[11] Wang S X and Zhang H 2003 *Phys. Rev.* B **68** 012503
[12] Rietveld H M 1969 *J. Appl. Crystallogr.* **2** 65
[13] Fehrenbacher R and Rice T M 1993 *Phys. Rev. lett.* **70** 3471
[14] Fink J, Nücker N, Romberg H, Alexander M, Maple M B, Neumeier J J and Allen J W 1990 *Phys. Rev.* B **42** 4823
[15] Merz M, Nücker N, Pellegrin E, Schweiss P, Schuppler S, Kielwein M, Knupfer M, Golden M S, Fink J, Chen C T, Chakarian V, Idzerda Y U and Erb A 1997 *Phys. Rev.* B **55** 9160
[16] Renevier H, Hodeau J L, Marezio M and Santoro A 1994 *Physica* C **2** 143
[17] Kulkarni R G, Kuberkar D G, Baldha G J and Bichile G K 1993 *Physica* C **217** 175
[18] Xu Y W, Kramer M J, Dennis K W, Wu H, O'Connor A, McCallum R W, Malik S K and Yelon W B 2000 *Physica* C **333** 195
[19] Kini N S and Umarji A M 2003 *Solid State Sci.* **5** 1451
[20] Tan W S and Wu X S 2001 *J. Supercond.: Inc. Novel Magn.* **14** 525
[21] Cava R J, Batlogg B, Fleming R M, Sunshine S A, Ramirez A, Rietman E A, Zahurak S M and van Dover R B 1988 *Phys. Rev.* B **37** 5912
[22] Jorgensen J D, Beno M A, Hinks D G, Soderholm L, Volin K J, Hitterman R L, Grace J D, Schuller I K, Segre C U, Zhang K and Kleefisch M S 1987 *Phys. Rev.* B **36** 3608
[23] Tu K N, Yeh N C, Park S I and Tsuei C C 1989 *Phys. Rev.* B **39** 304

[24] Rodriguez M A, Snyder R L, Chen B J, Matheis D P, Misture S T and Frechette V D 1993 *Physica* C **206** 43
[25] Crawford M K, Harlow R L, McCarron E M, Farneth W E, Axe J D, Chou H and Huang Q 1991 *Phys. Rev.* B **44** 7749
[26] Koike Y, Kobayashi A, Kawaguchi T, Kato M, Noji T, Ono Y, Hikita T and Saito Y 1992 *Solid State Commun.* **82** 889
[27] Akoshima M, Noji T, Ono Y and Koike Y 1998 *Phys. Rev.* B **57** 7491